

# 1 Short-term origin-destination demand prediction in urban rail transit systems: 2 A channel-wise attentive split-convolutional neural network method

3 Jinlei Zhang<sup>a</sup>, Hongshu Che<sup>c</sup>, Feng Chen<sup>b, d, \*</sup>, Wei Ma<sup>e</sup>, Zhengbing He<sup>f</sup>

4 <sup>a</sup> State Key Laboratory of Rail Traffic Control and Safety, Beijing Jiaotong University, Beijing 100044, China

5 <sup>b</sup> School of Civil Engineering, Beijing Jiaotong University, Beijing 100044, China

6 <sup>c</sup> School of Automation, Southeast University, Nanjing, 211189, China

7 <sup>d</sup> Beijing General Municipal Engineering Design and Research Institute Company Ltd., Beijing 100082, China

8 <sup>e</sup> Department of Civil and Environmental Engineering, The Hong Kong Polytechnic University, Hong Kong SAR, China

9 <sup>f</sup> Beijing Key Laboratory of Traffic Engineering, Beijing University of Technology, Beijing 100124, China

10 \* Correspondence: fengchen@bjtu.edu.cn

11

12

13

## 14 Abstract

15

16 Short-term origin-destination (OD) flow prediction in urban rail transit (URT) plays a crucial role in smart  
17 and real-time URT operation and management. Different from other short-term traffic forecasting  
18 methods, the short-term OD flow prediction possesses three unique characteristics: 1) data availability:  
19 real-time OD flow is not available during the prediction; 2) data dimensionality: the dimension of the OD  
20 flow is much higher than the cardinality of transportation networks; 3) data sparsity: URT OD flow is  
21 spatiotemporally sparse. There is a great need to develop novel OD flow forecasting method that explicitly  
22 considers the unique characteristics of the URT system. To this end, a channel-wise attentive split-  
23 convolutional neural network (CAS-CNN) is proposed. The proposed model consists of many novel  
24 components such as the channel-wise attention mechanism and split CNN. **In particular, an  
25 inflow/outflow-gated mechanism is innovatively introduced to address the data availability issue.** We  
26 further originally propose a masked loss function to solve the data dimensionality and data sparsity issues.  
27 The model interpretability is also discussed in detail. The CAS-CNN model is tested on two large-scale  
28 real-world datasets from Beijing Subway, and it outperforms the rest of benchmarking methods. The  
29 proposed model contributes to the development of short-term OD flow prediction, and it also lays the  
30 foundations of real-time URT operation and management.

31

32 *Keywords:* Deep learning; Urban rail transit; Short-term origin-destination prediction; Channel-wise  
33 attention; Split CNN

34

35

36

## 37 1 Introduction

38 In recent years, the urban rail transit (URT) has experienced rapid expansion. Significant  
39 attention has been devoted to its intelligent operation and management. As one of the  
40 fundamental tasks of intelligent transportation systems, short-term passenger flow  
41 prediction has attracted increasing research interest because of its practical influence on  
42 both passengers and operators (Liu *et al.*, 2020). **For operators, the result of OD prediction  
43 can help to better monitor the real-time spatiotemporal distribution of passenger flows,  
44 thus supporting decisions on network management tasks, such as implement congestion  
45 control and anomaly detection. Real-time measures, such as the adjustment of train  
46 timetables (shortening or extending the headway), can be taken to avoid congestions and  
47 save operational costs. If the congestion or large passenger flow is monitored, operators**

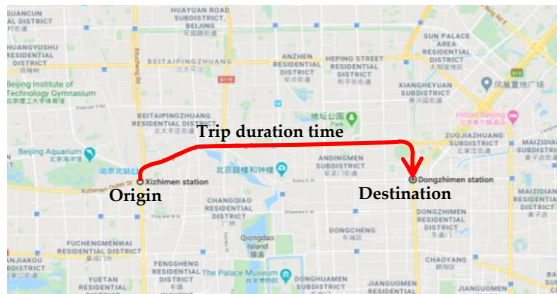
48 can reasonably allocate staff members to evacuate passengers, thus avoiding or improving  
49 the accident situation. Moreover, for passengers, an accurate short-term prediction is  
50 beneficial to route scheduling that saves travel time and thus improves travel experience.

51 Network-scale short-term passenger flow prediction systems for URT can be  
52 categorized into inflow prediction, origin-destination (OD) passenger flow prediction, and  
53 sectional passenger flow prediction (Zhang *et al.*, 2019). Short-term inflow prediction,  
54 which refers to the forecast of passenger demands entering each station, has been  
55 extensively studied (Han *et al.*, 2019, Liu *et al.*, 2019, Wei and Chen, 2012, Zhang *et al.*, 2019,  
56 Zhang *et al.*, 2020, Zhang *et al.*, 2020a). After obtaining the real-time inflow, that is, the  
57 passenger origins, short-term OD flow prediction can be conducted to forecast passenger  
58 destinations (Vlahogianni *et al.*, 2014). Lastly, the sectional passenger flow prediction task  
59 refers to the forecast of the specific path chosen by passengers in order to arrive at  
60 destinations from origins. Because the individual's trajectory is difficult to obtain in URT,  
61 the sectional passenger flow is usually obtained by leveraging transit assignment models  
62 to estimate the travelers' behaviors using OD matrices as essential inputs. Overall, OD flow  
63 prediction is the bridge between inflow prediction and sectional passenger flow prediction,  
64 and it plays a crucial role in the network-scale short-term passenger flow prediction  
65 systems. An accurate OD flow prediction model can provide the spatiotemporal mobility  
66 patterns among subway stations, thus contributing to a better understanding of travel  
67 behaviors (Xiong *et al.*, 2019). Therefore, this paper focuses on the short-term OD passenger  
68 flow prediction in URT.

69 Short-term network-wise traffic prediction has been studied extensively over the past  
70 decades. Various data-driven and model-based prediction methods have been developed  
71 to forecast road speed/flow, road OD demand, ride-hailing demand, ride-hailing OD  
72 demand, and URT inflow/outflow. To the best of our knowledge, there are few studies on  
73 the short-term URT OD passenger flow prediction, as there exist several characteristics  
74 that distinguish OD prediction tasks in URT from the rest of prediction tasks. These  
75 characteristics can be listed as follows:

- 76 1. **Data availability.** In most of the short-term traffic forecasting problems, the real-  
77 time traffic data can be obtained in time. For example, in the traffic speed  
78 prediction task, we can obtain the real-time traffic speed at time  $t$  in order to  
79 predict the speed at time  $t+1$ . Similarly, the URT inflow/outflow can be obtained  
80 in real-time because passengers must swipe cards when they enter subway  
81 stations. The card swiping information can be aggregated in real-time and the  
82 inflow/outflow at each URT station can be computed. For this type of tasks, the  
83 actual traffic states in the last several time intervals can be used as model inputs  
84 when short-term traffic forecast is conducted. However, URT OD flows cannot be  
85 obtained in real-time because there is always trip duration time from the origin to  
86 the destination, as shown in Fig. 1. The OD matrix can only be obtained when all  
87 the travelers finish their trips. Therefore, when conducting real-time URT OD  
88 predictions, the model inputs should be carefully considered. One noteworthy  
89 point is that the model input for real-time road OD demand prediction is usually

90 the road traffic volumes, which can be obtained in real-time (Xiong et al., 2019).  
 91 The real-time ride-hailing OD demand can also be obtained in real-time as users  
 92 need to identify the origin and destination when they start to use the services (Ke  
 93 *et al.*, 2019). In addition, for the URT data, the inflow/outflow volume is always  
 94 equal to the sum of OD flows as all passengers will eventually exit the stations.



95  
 96 Fig. 1. Diagram of trip duration time of the OD pair

- 97 2. **Data dimensionality.** The number of OD flows is  $n^2$  times the number of stations,  
 98 where  $n$  is the number of URT stations. This tremendously increases the difficulty  
 99 in the prediction of OD flows. For example, there are 404 URT stations in Beijing,  
 100 meaning the dimensionality of OD flow in Beijing is 163,216. Similarly, there are  
 101 270 stations in London and 424 stations in New York, and hence the  
 102 dimensionality of OD flow is much larger than the cardinality of the  
 103 transportation networks.
- 104 3. **Data sparsity.** The URT OD flow is spatiotemporally sparse, meaning that there  
 105 is no passenger flow for many OD pairs. The reasons are two-fold: 1) the travel  
 106 patterns change over time, leading to the time-varying sparse patterns of OD flows.  
 107 For example, most OD flows depart from residual areas and arrive in the  
 108 commercial areas in the morning peak hours, and the flow is reversed during the  
 109 afternoon peak hours; 2) due to the large dimensionality of OD flow, the total  
 110 travel demand disperses over different OD pairs, making many OD flows either  
 111 small or zero. Fig. 2 presents the OD pairs from a downtown station (A) to suburb  
 112 stations (B, C, D, E) in Beijing, and we can read from the data that there are  
 113 generally small or zero OD flows between  $A \rightarrow B$ ,  $A \rightarrow C$ ,  $A \rightarrow D$ , and  $A \rightarrow E$  in the  
 114 morning because few passengers go from downtown to suburb during morning  
 115 peak hours. Table 1 shows the proportion of different OD flows in specific time  
 116 intervals. There are more than 40% OD pairs with zero flow throughout the day.  
 117 OD flows fewer than two account for more than 65% throughout the day. These  
 118 small or zero OD flows are usually attributed to randomly generated trips that  
 119 significantly decrease the regularity of OD flows, and thus increase the prediction  
 120 difficulty. OD predictions for road traffic and ride-hailing service also suffers data  
 121 sparsity issue while they are not as serious as that of URT, due to the availability  
 122 of the real-time information. In contrast, the corresponding URT inflow/outflow,  
 123 road flow, and ride-hailing demand are dense, and the volume is relatively large.

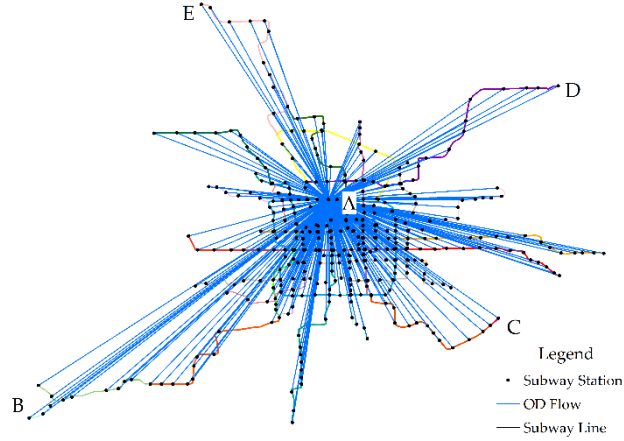


Fig. 2. Diagram of OD flows in Beijing, China

Table 1 OD flow statistics in OD matrix in Beijing, China

OD flow	05:00–05:30	08:00–08:30	12:00–12:30	19:00–19:30
OD = 0	95.16%	40.53%	58.46%	54.92%
$0 < OD \leq 2$	4.34%	25.21%	27.57%	25.41%
$2 < OD \leq 4$	0.34%	10.40%	7.89%	8.22%
$4 < OD \leq 6$	0.09%	5.74%	2.87%	3.77%
OD > 6	0.07%	18.12%	3.21%	7.68%

Table 2 summarizes the characteristics of different traffic state forecasting methods. As can be seen, the URT OD flow prediction task is the only task that requires careful design of model inputs, and the data dimensionality and sparsity issues also present. Given the valuable information in the URT OD flow, there is a lack of study on the short-term forecasting methods for the OD passenger flow for URT.

Table 2 Summary of the characteristics of different traffic state forecasting methods

	Data Availability	Data Dimensionality	Data Sparsity	References
Road Speed/Flow	✓	✓	✓	(Guo <i>et al.</i> , 2019, Ma <i>et al.</i> , 2015)
Road OD Flow	✓	!	!	(Xiong <i>et al.</i> , 2019)
Ride-hailing Demand	✓	✓	✓	(Geng <i>et al.</i> , 2019)
Ride-hailing OD Demand	✓	!	!	(Ke <i>et al.</i> , 2019)
URT Inflow/outflow	✓	✓	✓	(Zhang <i>et al.</i> , 2020)
URT OD Flow	!	!	!	This study

Note: “✓” denotes issue not present and “!” denotes issue present.

In summary, this study is motivated by several issues to be addressed in short-term OD prediction in URT.

1. First, real-time OD matrices are unavailable. It is impractical to use OD matrices in the last several time intervals as model inputs. Hence, determining the inputs is the first problem to be tackled when conducting real-time OD prediction.
2. Second, existing studies generally ignore the relationship between inflow/outflow and OD flows in URT. Thus, their relationship should be explicitly modeled in the

142 prediction models.

143 3. Third, most studies treat OD pairs with large flows and small flows equally, which  
144 can significantly reduce the prediction accuracy as there are many OD pairs with  
145 even no flow. The data sparsity issue is critical for OD flow prediction. Therefore,  
146 how to address the data sparsity to improve the prediction accuracy is another  
147 crucial problem.

148 4. Finally, in general, state-of-the-art deep-learning models are becoming  
149 increasingly complicated to improve prediction accuracy. However, the important  
150 question is whether increased complexity is better. This is another issue that needs  
151 to be explored.

152 In view of this, this paper introduces a channel-wise attentive split convolutional  
153 neural network (CAS-CNN) model to address these problems. In the proposed model, an  
154 inflow/outflow-gated mechanism is originally introduced to aggregate historical OD flow  
155 information and real-time inflow/outflow information, which solves the data availability  
156 issue. A split CNN is proposed for the first time in short-term OD prediction to combine  
157 sparse OD data and convert to dense features. Moreover, a masked loss function is  
158 introduced and justified mathematically to address the data dimensionality and sparsity  
159 issues. A channel-wise attention mechanism is applied to score the inputs as well as the  
160 extracted high-level features. Experiments on two real-world datasets from the Beijing  
161 subway show the superiority of the CAS-CNN model. The main contributions are  
162 summarized as follows:

- 163 1. The characteristics of URT OD prediction and the comparisons with other traffic  
164 forecasting tasks are summarized in detail. The problems of the short-term OD  
165 prediction in URT are also summarized.
- 166 2. An inflow/outflow-gated mechanism is developed to aggregate historical OD flow  
167 information and real-time inflow/outflow information by considering their  
168 intrinsic dependency.
- 169 3. A split CNN model is introduced to convert the sparse OD flow information to  
170 dense and useful features. To the best of our knowledge, this is the first time that  
171 the split CNN is introduced in short-term OD predictions.
- 172 4. A masked loss function is proposed based on the OD attraction degree (ODAD)  
173 indicator to handle small or zero OD flows.

174 The remaining sections are organized as follows. Section 2 reviews the literature. The  
175 methodology is described in Section 3. The experimental details and results are presented  
176 in Section 4, and the conclusions are summarized in Section 5.

## 177 2 Literature review

### 178 2.1 Traffic inflow and outflow predictions

179 Research studies on traffic inflow and outflow predictions have been prevailing in recent  
180 years, and the adopted methods range from conventional statistical methods to artificial-  
181 intelligence-based methods. The latter has been proved to be more effective in real-world

182 applications owing to the massive mobility data that has been collected in recent decades,  
183 as well as the emerging deep-learning techniques. Since the long short-term memory  
184 (LSTM) was first introduced in the traffic prediction field in 2015 (Ma *et al.*, 2015), many  
185 deep-learning models have been proposed, such as the classical CNN (Ma *et al.*, 2017),  
186 stacked autoencoder (Lv *et al.*, 2015), ST-ResNet (Zhang *et al.*, 2017), and ST-GCN (Yu *et al.*,  
187 2017), as well as the latest hybrid models that combined two or more RNNs, CNNs, and  
188 GCNs, such as ResLSTM (Zhang *et al.*, 2020), RSTN (Guo and Zhang, 2020), SBU-LSTM  
189 (Cui *et al.*, 2020), Conv-GCN (Zhang *et al.*, 2020b), TGC-LSTM (Cui *et al.*, 2019), GATCN  
190 (Guo and Yuan, 2020), and GA-LSTM (Zhang and Guo, 2020). Recently, the transformer  
191 (Xu *et al.*, 2020), the generative adversarial (Zhang *et al.*, 2019), and the capsule networks  
192 (Ma *et al.*, 2020) are also utilized for short-term predictions. Among these models, some are  
193 used for short-term predictions whereas others are for medium- or long-term predictions  
194 (Li *et al.*, 2018, Sun and Chen, 2019). Some are for single or several subway stations (Liu *et al.*,  
195 2019, Zhang *et al.*, 2019), whereas others are for network-wide predictions. Some are  
196 for predictions under normal conditions (Xu *et al.*, 2020, Jin *et al.*, 2020), whereas others are  
197 for abnormal conditions (Yu *et al.*, 2020). Some are for predictions using stationary  
198 correlations (Chai *et al.*, 2018), whereas others are for predictions using dynamic  
199 correlations (Yao *et al.*, 2019).

200 Overall, many types of models are built to accommodate various scenarios. However,  
201 all of them are for inflow or outflow predictions and are critically different from OD  
202 prediction in terms of data availability, data dimensionality, and data sparsity as  
203 mentioned in the introduction section. Therefore, it is necessary to build forecasting  
204 models that explicitly consider the unique characteristics of URT OD flows.

## 205 **2.2 Traffic OD prediction and estimation**

206 Due to the data dimensionality and sparsity issues, obtaining accurate OD demand is  
207 much more challenging than obtaining the inflow or outflow, regardless of whether the  
208 OD demand is road demand, ride-hailing demand, or URT demand.

209 Traffic OD prediction is different from inflow or outflow predictions, as mentioned in the  
210 introduction section. In terms of the prediction methods and the research objects, we have  
211 divided related studies into several categories as follows.

212 In terms of the methods, OD matrix prediction and estimation can be categorized into  
213 three categories. The first category is the conventional methods, such as the least-squares  
214 estimation algorithm (Yao *et al.*, 2016) and probability analysis model (Wang *et al.*, 2011).  
215 The second category is the machine learning method, such as the state space model (Yao  
216 *et al.*, 2015, Lin and Chang, 2007), back-propagation neural network (Zhou *et al.*, 2016),  
217 principal component analysis and singular value decomposition (Yang *et al.*, 2017), and  
218 hierarchical Bayesian networks (Ma *et al.*, 2013). However, there are some common  
219 shortcomings among these two categories. First, these methods cannot meet the real-time  
220 requirements. For example, when applied to large-scale networks, the least-squares  
221 method and state space model consume considerable computational resources, making  
222 them practically inapplicable. Second, the prediction accuracy needs to be improved. Third,

223 the spatial and temporal correlations of the OD demand can hardly be considered.

224 To tackle these problems, deep-learning methods, which belong to the third category,  
225 have been developed extensively in recent years. Some researchers used the LSTM model  
226 to conduct the OD matrix prediction (Xi *et al.*, 2018). Each node is trained to obtain a  
227 specific LSTM model with the use of the parallel computing technique. However, this  
228 method cannot capture spatial correlations among all the OD pairs. Some studies applied  
229 CNN and GCN (Liu *et al.*, 2019, Wang *et al.*, 2019) to perform OD matrix prediction. These  
230 studies were applied to road traffic paradigms, in which the origin and destination zones  
231 are significantly different from the subway systems. Some studies (Xiong *et al.*, 2019) also  
232 leveraged GCN to perform OD matrix prediction in road traffic paradigms in which links  
233 were treated as nodes and the adjacent matrix represented link connections. Destination  
234 prediction in the bike-sharing system was also explored by combining LSTM and CNN  
235 (Jiang *et al.*, 2019), while fewer bike stations could significantly reduce the problem  
236 difficulty comparing to the URT system. Overall, the contextual information of the above  
237 mentioned deep-learning studies is different from that of URT, while they can still provide  
238 intuition and implications for developing the deep learning model for URT OD flow  
239 prediction.

240 In terms of research objects, short-term OD matrix prediction or estimation can be  
241 divided into road OD estimation (Lin and Chang, 2007), taxi OD matrix prediction (Ou *et al.*,  
242 2019, Liu *et al.*, 2019, Wang *et al.*, 2019), bus OD matrix prediction (Zhang *et al.*, 2017),  
243 and URT OD matrix prediction (Yang *et al.*, 2017, Yao *et al.*, 2016, Yao *et al.*, 2015, Wang *et al.*,  
244 2011, Zhao *et al.*, 2007). The data available is different for different objects. In the road  
245 network, neither the real-time nor the true OD matrices cannot be obtained. However, the  
246 sectional link counts can be observed. Thus, the road OD matrix can be estimated via  
247 optimization models such as the bi-level programming model. Notably, it is difficult to  
248 evaluate the reliability of the estimated OD matrix because there is no true OD matrix for  
249 comparison (Yang *et al.*, 1991). In the case of the taxi OD matrix, because there are no fixed  
250 boarding and alighting points, existing methods always partition the entire research area  
251 to construct origin and destination regions (Traffic Analysis Zones or TAZs). In this case,  
252 the true OD matrix between TAZs can be obtained, whereas the real-time counterparts  
253 cannot. In the bus system, existing studies focus on one or several lines to conduct OD  
254 matrix prediction because the bus network is critically large-scale. Furthermore, data  
255 availability issue varies in different bus systems, as some bus systems can record boarding  
256 and alighting stations, whereas some can only record the boarding station. In URT, there  
257 are fixed subway stations, and passengers must swipe cards when they enter and exit  
258 stations. Therefore, the true OD matrix can be obtained based on historical smart card data.  
259 However, as discussed in the previous section, the real-time counterparts cannot be  
260 obtained because of the trip duration time.

261 Specifically, in URT, the OD matrix prediction studies that use deep-learning methods  
262 are critically few. Several existing studies built state space models (Chen *et al.*, 2017, Yao *et al.*  
263 *et al.*, 2015) or least-squares methods (Yao *et al.*, 2016). Notably, a recent study applied the  
264 LSTM to perform OD matrix prediction in which a specific LSTM model was specifically

265 trained for each of all the subway stations leveraging parallel computing techniques  
266 (Zhang et al., 2019). However, these studies exhibit some drawbacks. For example, they  
267 cannot capture complicated spatiotemporal correlations and nonlinear characteristics  
268 among OD flows. Moreover, each URT station requires to train a deep learning model  
269 separately, making the method computationally infeasible because there are many subway  
270 stations.

## 271 **2.3 Summary**

272 In order to contribute to the literature of short-term OD demand prediction, two main  
273 issues should be addressed for the URT system. Overall, the principle is that unique  
274 models should be developed because of the unique characteristics of the URT system. The  
275 detailed discussions are as follows:

- 276 (1) Deep learning methods have certain advantages over conventional methods. Many  
277 studies have demonstrated that deep learning methods can meet the real-time  
278 requirements as well as have high prediction accuracy. Moreover, it is feasible to train  
279 only one model for all stations. Therefore, developing deep-learning models to conduct  
280 OD prediction in URT is in real need.
- 281 (2) Due to the data availability issue, two types of information are available: OD demand  
282 in previous days and the real-time inflow/outflow. Hence it is critically important to  
283 combine the information of both data.
- 284 (3) The OD matrices are critically sparse and the dimension is large, especially in a large  
285 subway network. A systemic way needs to be developed to account for the sparsity  
286 level of different OD pairs and large dimensions of OD matrices.

## 287 **3 Methodology**

288 In this section, we formulate the methodological architecture. First, the problem of short-  
289 term OD prediction in URT is defined, and an indicator called the ODAD is introduced.  
290 The model architecture is then developed, followed by the introduction of the split CNN,  
291 the channel-wise attention mechanism, and the inflow/outflow-gated mechanism.

### 292 **3.1 Problem definition**

293 The goal of this study is to predict the OD matrix in the next time interval using historical  
294 information. The time interval is defined as 30 min in this study. The OD matrix  $M$  and  
295 inflow/outflow  $N$  can be extracted from smart card data in URT, and can be defined  
296 according to Eqs. (1) to (3). Notably, the OD flow of each time interval depends on the time  
297 interval in which the passengers enter the stations, as the exit time of each passenger might  
298 differ. The inflow/outflow series is extracted according to the corresponding entry station,  
299 entry time, exit station, and exit time.



$$M^{d,t} \in \mathbb{R}^{n \times n} = \begin{pmatrix} m_{11}^{d,t} & m_{12}^{d,t} & m_{13}^{d,t} & \cdots & m_{1j}^{d,t} \\ m_{21}^{d,t} & m_{22}^{d,t} & m_{23}^{d,t} & \cdots & m_{2j}^{d,t} \\ m_{31}^{d,t} & m_{32}^{d,t} & m_{33}^{d,t} & \cdots & m_{3j}^{d,t} \\ \vdots & \vdots & \vdots & \ddots & \vdots \\ m_{i1}^{d,t} & m_{i2}^{d,t} & m_{i3}^{d,t} & \cdots & m_{ij}^{d,t} \end{pmatrix} \quad (1)$$

$$N^{d,t} \in \mathbb{R}^{n \times t} = \begin{pmatrix} n_1^{d,1} & n_1^{d,2} & n_1^{d,3} & \cdots & n_1^{d,t} \\ n_2^{d,1} & n_2^{d,2} & n_2^{d,3} & \cdots & n_2^{d,t} \\ n_3^{d,1} & n_3^{d,2} & n_3^{d,3} & \cdots & n_3^{d,t} \\ \vdots & \vdots & \vdots & \ddots & \vdots \\ n_i^{d,1} & n_i^{d,2} & n_i^{d,3} & \cdots & n_i^{d,t} \end{pmatrix} \quad (2)$$

$$\begin{pmatrix} n_1^{d,t} \\ n_2^{d,t} \\ n_3^{d,t} \\ \vdots \\ n_i^{d,t} \end{pmatrix} = \begin{pmatrix} \sum_j m_{1j}^{d,t} \\ \sum_j m_{2j}^{d,t} \\ \sum_j m_{3j}^{d,t} \\ \vdots \\ \sum_j m_{ij}^{d,t} \end{pmatrix}, \quad n_i^{d,t} = \sum_j m_{ij}^{d,t} \text{ (inflow), or} \quad (3)$$

$$\begin{pmatrix} n_1^{d,t} \\ n_2^{d,t} \\ n_3^{d,t} \\ \vdots \\ n_i^{d,t} \end{pmatrix} = \begin{pmatrix} \sum_i m_{i1}^{d,t} \\ \sum_i m_{i2}^{d,t} \\ \sum_i m_{i3}^{d,t} \\ \vdots \\ \sum_i m_{ij}^{d,t} \end{pmatrix}, \quad n_i^{d,t} = \sum_i m_{ij}^{d,t} \text{ (outflow)}$$

303 where  $m_{ij}^{d,t}$  represents the OD flow from station  $i$  to station  $j$  in the time interval  $t$  on day

304  $d$ .  $\sum_j m_{ij}^{d,t}$  is the sum of OD flows that enter station  $i$  in the time interval  $t$  on day  $d$ , and

305  $n_i^{d,t}$  is the inflow/outflow entering/exiting station  $i$  in the time interval  $t$  on day  $d$ . The

306 stations are ordered according to their adjacency in the subway line. Notably, there are

307 inherent correlations between inflow/outflow and OD flows, as shown in Eq. (3). The

308 inflow/outflow equals to the sum of corresponding OD flows in each row/column.

309 Regarding short-term OD prediction, prior studies generally used the OD matrices in

310 the last several time intervals as model inputs to predict the OD matrix in the subsequent

311 time interval (Liu et al., 2019, Wang et al., 2019). However, the real-time OD matrix cannot

312 be obtained because of the trip duration time. Therefore, these studies cannot be applied

313 for real-time operations. Similarly, in the real-time operation of URT, the real-time OD

314 matrix cannot be obtained. However, real-time inflow/outflow is available. Therefore, this

315 study seeks to predict the short-term OD matrix using the OD matrix of the previous

316 several days, as well as the inflow/outflow of the same day, as expressed by Eq. (4).

317 
$$M^{d,t} = f(\{M^{d-x,t}\}_x, \{N^{d,t-y}\}_y), x = 1, 2, 3 \dots; y = 1, 2, 3 \dots \quad (4)$$

318 where  $M^{d,t}$  is the OD matrix in the time interval  $t$  on day  $d$ . One of the inputs is the OD  
 319 matrix  $M^{d-x,t}$  in the same time interval  $t$  during the last several days  $d-x$ . Another input  
 320 is the inflow/outflow series  $N^{d,t-y}$  during the last several time intervals  $t-y$  of the same  
 321 day  $d$ . Because the real-time OD matrix is not available, we innovatively designed an  
 322 inflow/outflow -gated mechanism with the real-time inflow as inputs to provide real-time  
 323 information.

324 **3.2 Origin–destination attraction degree (ODAD) level**

325 To characterize OD flows with different volumes, we introduce a novel indicator  
 326 called ODAD (Zhang et al., 2019). It is defined as the average OD flow in a specific time  
 327 interval during a longer period, as indicated by Eq. (5).

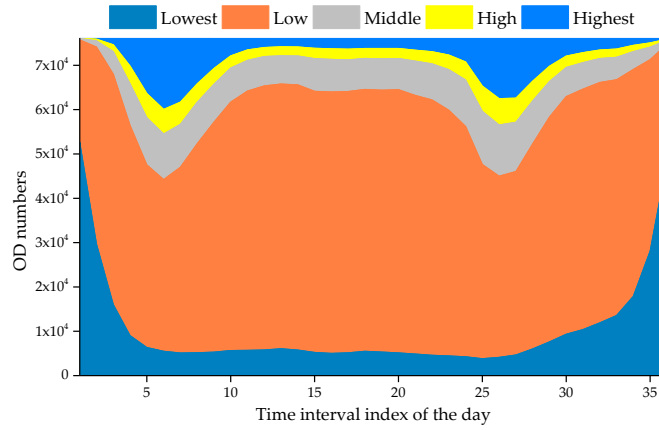
328 
$$\text{ODAD}^t = \begin{pmatrix} a_{11}^t & a_{12}^t & a_{13}^t & \cdots & a_{1j}^t \\ a_{21}^t & a_{22}^t & a_{23}^t & \cdots & a_{2j}^t \\ a_{31}^t & a_{32}^t & a_{33}^t & \cdots & a_{3j}^t \\ \vdots & \vdots & \vdots & \ddots & \vdots \\ a_{i1}^t & a_{i2}^t & a_{i3}^t & \cdots & a_{ij}^t \end{pmatrix}, a_{ij}^t = \frac{1}{n} \sum_{d=1}^n a_{ij}^{d,t} \quad (5)$$

329 where  $a_{ij}^t$  is the average OD flow from station  $i$  to station  $j$  during an  $n$ -day period. It is a  
 330 dynamic indicator that varies with time. For a specific OD pair, the  $a_{ij}^t$  value may be low  
 331 early in the morning and high during peak hours. It is also an average indicator used to  
 332 avoid randomness.

333 To handle OD pairs with different attraction degrees, we divide all OD pairs into five  
 334 levels according to their ODAD values, as shown in Table 3. The variation of OD numbers  
 335 at different ODAD levels is shown in Fig. 3. A sub-OD matrix in a single time interval is  
 336 shown in Fig. 4. Temporally, the OD pairs at low and lowest levels account for a large  
 337 majority. Spatially, OD flows only occur in specific areas. These small values negatively  
 338 affect the model performance because the lack of regularity increases the difficulty to make  
 339 predictions. Therefore, it is challenging to handle these small or zero values. To solve this  
 340 problem, we innovatively introduce a masked loss function according to the “low” ODAD  
 341 level in Section 3.7, thus reducing the impact of small or zero OD flows on the prediction  
 342 accuracy. The “low” ODAD level used in this study is fixed and does not change with time.

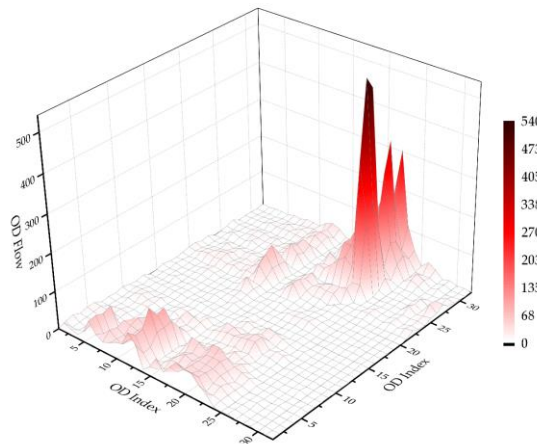
343 Table 3 OD attraction degree (ODAD) level definition

ODAD value	$a_{ij}^t = 0$	$0 < a_{ij}^t \leq 2$	$2 < a_{ij}^t \leq 4$	$4 < a_{ij}^t \leq 6$	$a_{ij}^t > 6$
ODAD level	Lowest	Low	Middle	High	Highest



344  
345

Fig. 3. Variation of OD numbers in a single day



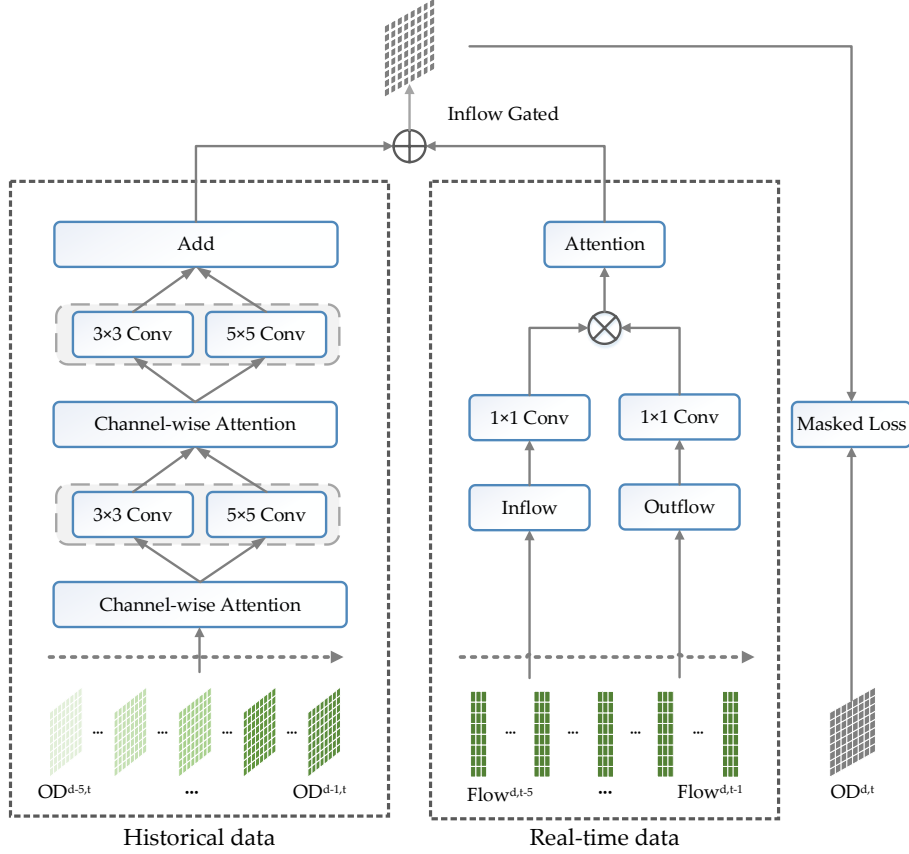
346  
347

Fig. 4. Three-dimensional (3D) view of a sub-OD matrix

### 3.3 Model development

348

349 We propose the prediction framework based on the split CNN, channel-wise attention, and  
 350 inflow/outflow -gated mechanism (referred to as CAS-CNN as shown in Fig. 5) to conduct  
 351 short-term OD prediction in URT. The CAS-CNN comprises two branches for historical  
 352 data and real-time data, respectively.



353

354

Fig. 5. Model architecture for CAS-CNN

355

In the branch of the historical data (short as trunk), we originally introduce a split CNN to capture spatiotemporal correlations with different perceptive fields, as well as to produce dense information from sparse OD flows. The channel-wise attention is used to weight the inputs, and different high-level features are extracted from the OD matrix. To the best of our knowledge, this is the first time that the split CNN is applied to URT OD prediction.

361

In the branch of real-time information, we use real-time inflows/outflows as inputs to extract important information. To merge the two sources of data, an ingenious inflow/outflow-gated mechanism is designed to aggregate historical OD flow information and real-time inflow/outflow information by considering their intrinsic dependency.

365

To address small and zero OD flows, we also introduce a masked loss function based on the low ODAD level.

367

In the following sections, the split CNN, channel-wise attention, inflow/outflow-gated mechanism, and the masked loss function are described in detail.

369

### 3.4 Split CNN

370

Existing studies generally use one same-size kernel to extract features (Ma et al., 2017, Zhang et al., 2020, Liu et al., 2019). In this case, to improve the training performance, a general method is to increase the network depth (number of layers). However, the increase in the number of layers has multiple undesirable effects, such as overfitting, vanishing gradient, gradient explosion, etc. Although the residual network (He *et al.*, 2015) has been

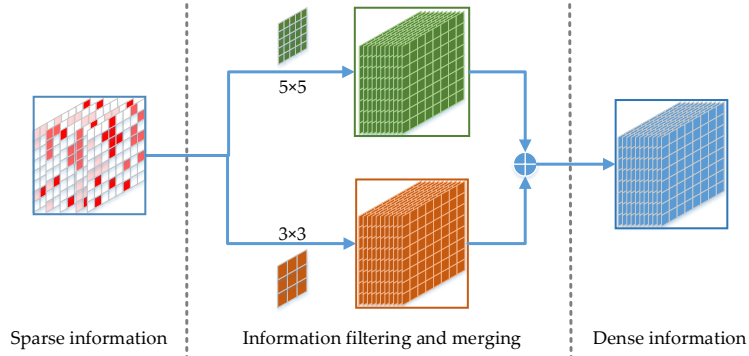
374

375 proposed to solve these problems, it also increases network complexity and computational  
 376 resources such as the training time.

377 Motivated by GoogLeNet (Szegedy *et al.*, 2015, Szegedy *et al.*, 2016), in this study, we  
 378 originally introduce a split CNN model to address the task of short-term OD prediction.  
 379 To the best of our knowledge, this is the first time that the split CNN is applied to short-  
 380 term OD prediction in URT. Rather than deepen the network, we choose to widen it with  
 381 different kernels, as shown in Fig. 6 and Fig. 7, as this can effectively increase the  
 382 adaptability of the network.

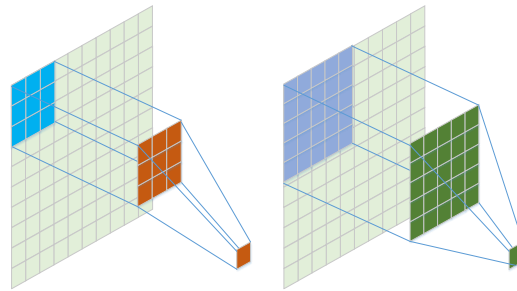
383 As mentioned above, one of the issues in short-term OD prediction in URT is data  
 384 sparsity. The split architecture is exactly suitable for OD matrices in URT because of the  
 385 serious data sparsity problem in two aspects.

386 Temporally, as shown in Table 1 and Fig. 3, OD flows at the “lowest” ODAD level  
 387 (namely, zero OD flows) are more than 40% throughout a day. By designing the split  
 388 architecture, dense data can be generated from relatively sparse matrices, and more  
 389 information can be extracted via different-size kernels. It cannot only increase the  
 390 performance of neural networks but also ensure the training efficiency.



391

392 Fig. 6. Diagram of split CNN (From sparse information to dense information)



393

394

Fig. 7. Diagram of the 3x3 and 5x5 kernels

395 Spatially, as shown in Fig. 4, only some specific areas exist OD flows. Therefore, in  
 396 flattened areas, a smaller kernel is adequate to capture its spatial characteristics. However,  
 397 in peak areas, a larger kernel is more suitable because it can capture more information with  
 398 the use of a larger perception field. In this case, some important information cannot be  
 399 easily omitted.

400 To this end, we introduce a split CNN for OD prediction in URT. The values  $v$  at  
 401 position  $(x, y)$  in the  $j^{th}$  feature map of the  $i^{th}$  layer can be calculated as follows (Zhang *et*  
 402 *al.*, 2020b).

$$v_{ij}^{xy} = \left( b_{ij} + \sum_m \sum_{p=0}^{P_i-1} \sum_{q=0}^{Q_i-1} w_{ijm}^{pq} v_{(i-1)m}^{(x+p)(y+q)} \right)_{k_1} + \left( b_{ij} + \sum_m \sum_{p=0}^{P_i-1} \sum_{q=0}^{Q_i-1} w_{ijm}^{pq} v_{(i-1)m}^{(x+p)(y+q)} \right)_{k_2} \quad (6)$$

where  $m$  denotes the index of the feature map in the  $(i-1)^{th}$  layer,  $w_{ijm}^{pq}$  is the  $(p, q)^{th}$  value of the kernel connected to the  $m^{th}$  feature map in the  $(i-1)^{th}$  layer,  $(P, Q)$  denotes the kernel dimension, and  $k$  denotes kernels with different sizes.

### 3.5 Channel-wise attention

The human-visual attention mechanism is a type of brain signal processing mechanism of human vision. By quickly scanning the global image, human vision acquires the target area that needs attention. Then, more attention resources are devoted to this area to obtain more detailed information about the target. Other useless information was suppressed simultaneously. This is a mechanism used by humans to quickly select high-value information from a large amount of information with limited attention resources. The human visual attention mechanism significantly improves the efficiency and accuracy of visual information processing.

Motivated by human visual attention, many types of attention mechanisms, such as self-attention and position-wise attention in Transformer (Vaswani *et al.*, 2017), residual attention (Wang *et al.*, 2017), multilayer attention (Yang *et al.*, 2016), and spatial attention (Chen *et al.*, 2017) have been proposed. The channel-wise attention mechanism was first proposed by (Chen *et al.*, 2017). It was used to weigh different high-level features, and can be applied in OD prediction for several aspects.

On the one hand, in the field of OD prediction in URT, the real-time OD matrix is not available. Therefore, we use the OD matrix in the same time interval of the last several days as one of the model inputs, as shown in Fig. 5. However, some of the OD matrices are highly related to the outputs. Some are lowly correlated to the outputs. It is taken for granted that the channel-wise attention can be used to weigh different OD inputs.

On the other hand, the output of split CNN represents high-level features extracted from inputs. It is important to adaptively focus more on some critical features to improve model performance. Therefore, we innovatively apply the channel-wise attention mechanism into the output of split CNN and add them together as shown in Fig. 8. Fig. 9 shows the details of channel-wise attention. There is a tensor reduction  $R$  during tensor processing used to represent nonlinear features. The output can thus be expressed as follows.

$$O^l = \left( \begin{array}{l} Y^l = CNN(X^l) \\ \delta_1 = \Phi(Y^l) \\ O_1^l = Y^l \times \delta_1 \end{array} \right)_{k_1} + \left( \begin{array}{l} Y^l = CNN(X^l) \\ \delta_2 = \Phi(Y^l) \\ O_2^l = Y^l \times \delta_2 \end{array} \right)_{k_2} \quad (7)$$

where  $\Phi$  represents the channel-wise attention operation,  $\delta$  is the attention vector, and  $k$  denotes different kernels.

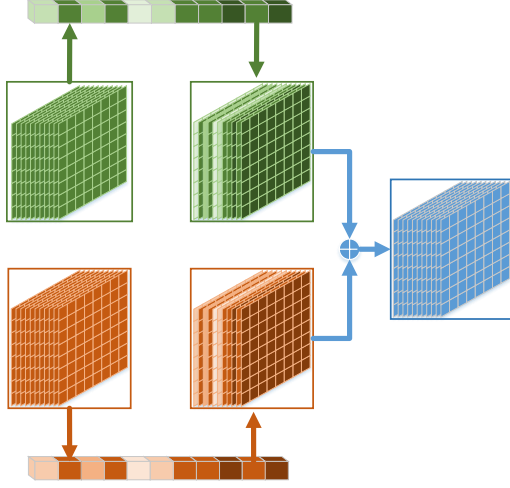


Fig. 8. Channel-wise attention after the split CNN

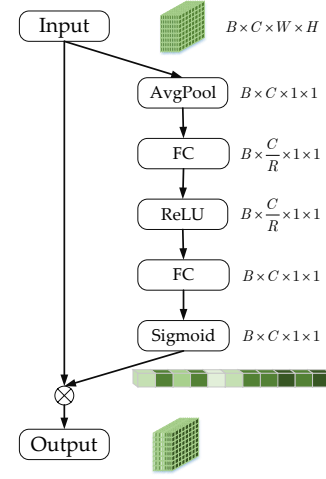


Fig. 9. Diagram of channel-wise attention

### 3.6 Inflow/outflow-gated mechanism

As is mentioned above, the real-time OD matrix is not available in URT. How to conduct OD predictions incorporating real-time information is dramatically important. As shown in Eqs. (1) to (3), there are strong correlations between inflows/outflows and OD flows. Motivated by the relationship, we originally introduce an inflow/outflow-gated mechanism to effectively control the trunk output and fuse the inflow/outflow and OD matrix information, as shown in Fig. 10. The inflow/outflow go through a  $1 \times 1$  convolutional layer. Their outputs are multiplied and then are weighted by an attention parameter vector. The weighted inflow features plus the output of the model trunk according to the rows is followed by a  $1 \times 1$  convolution to obtain the final predicted results.

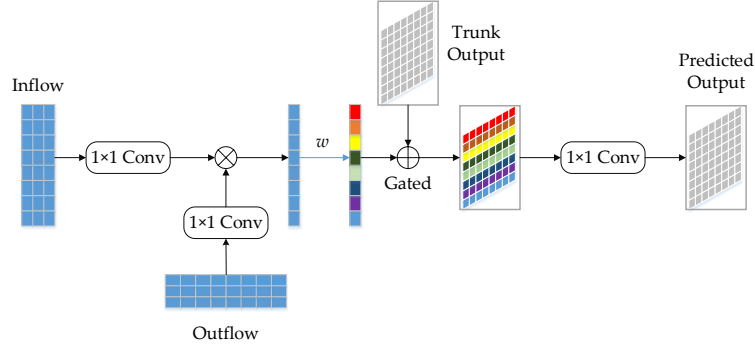


Fig. 10. Diagram of inflow/outflow-gated mechanism

The inflow/outflow  $N^{d,t} \in \mathbb{R}^{n \times t}$  in the last several time intervals is processed as follows.

$$\begin{aligned}
 O_{inflow/outflow} &= w \times CNN_{1 \times 1}(N_{inflow}) \times CNN_{1 \times 1}(N_{outflow}) \\
 O_{fuse} &= \left( O_{inflow/outflow} + O_{trunk} \right)_{by\ rows} \\
 O_{pre} &= CNN_{1 \times 1}(O_{fuse})
 \end{aligned} \tag{8}$$

where  $w$  is a column vector denoting the attention parameters of  $N_{inflow}$  and  $N_{outflow}$ , and  $O_{trunk}$  denotes the output of the model trunk. The variable  $w$  is used to model

456 interpretability analysis, as detailed in Section 4.3.3.

457 Notably, a  $1 \times 1$  convolutional layer is applied to obtain the final output. Each  $1 \times 1$   
 458 convolutional kernel can realize cross-channel information communication. The  $1 \times 1$  kernel  
 459 can replace the fully connected layer when nonlinear features are captured, while model  
 460 complexity is reduced. Therefore, although this denotes a simple linear combination, it is  
 461 conducive to information fusion and feature extraction.

### 462 3.7 Masked loss function

463 As discussed in previous sections, there are numerous small or zero OD flows that  
 464 significantly affect the prediction performance. Moreover, OD flows in different ODAD  
 465 levels are highly imbalanced both temporally and spatially, as shown in Table 1, Fig. 3, and  
 466 Fig. 4. Therefore, we introduce a masked loss function (M-Loss) as Eq. (9). We construct a  
 467 mask file according to the low ODAD level to mask the OD flows whose ODAD level are  
 468 less than two (Zhang et al., 2019).

$$469 \quad M\text{-Loss} = MSE = \frac{1}{(n \times n)_{no\_mask}} \sum_{i,j} mask \times (m_{ij}^{d,t} - m_{ij}^{d,t})^2 \quad (9)$$

470 where  $MSE$  is the masked mean-squared error,  $(n \times n)_{no\_mask}$  indicates the OD numbers  
 471 that are not masked,  $m_{ij}^{d,t}$  is the actual value and is the same as that in Eq. (1),  $m_{ij}^{d,t}$  is the  
 472 corresponding predicted value, and the  $mask$  is a matrix file, with values of zeros and ones,  
 473 which indicates whether the corresponding OD flows are masked or not. Because the  
 474 ODAD value changes with time for a specific OD pair, the mask file will be  
 475 correspondingly updated with time. It is noted that if the values are masked, the errors are  
 476 not backpropagated here, as proved in Eqs. (10) to (12), which can significantly improve  
 477 the prediction performance of OD flows that are not masked. The  $mask$  highlights the  
 478 import OD pairs, with higher traffic volumes. Only the errors of important flows (i.e. OD  
 479 flows with high volumes) will be backpropagated here. Assuming  $y = w \times x$ ,

$$480 \quad MSE = \frac{1}{(n \times n)_{no\_mask}} \sum_{i,j} mask \times (m_{ij}^{d,t} - w \times m_{ij}^{d,t})^2, \quad (10)$$

$$481 \quad gradient = \frac{\partial MSE}{\partial w} = \frac{-2 \times m_{ij}^{d,t}}{(n \times n)_{no\_mask}} \sum_{i,j} mask \times (m_{ij}^{d,t} - w \times m_{ij}^{d,t}), \quad (11)$$

$$482 \quad w_{new} = w - lr \times gradient = w + lr \times \frac{2 \times m_{ij}^{d,t}}{(n \times n)_{no\_mask}} \sum_{i,j} mask \times (m_{ij}^{d,t} - w \times m_{ij}^{d,t}). \quad (12)$$

483 If the value  $m_{ij}^{d,t}$  is masked, the corresponding  $mask$  is zero. Therefore,  $w_{new} = w$ , thus  
 484 indicating that the errors are not backpropagated.

## 485 4 Experiment

486 In this section, we test the proposed method with two real-world datasets and  
 487 compare it with benchmark methods. The experimental results are also analyzed from



488 multiple perspectives.

## 489 4.1 Data description

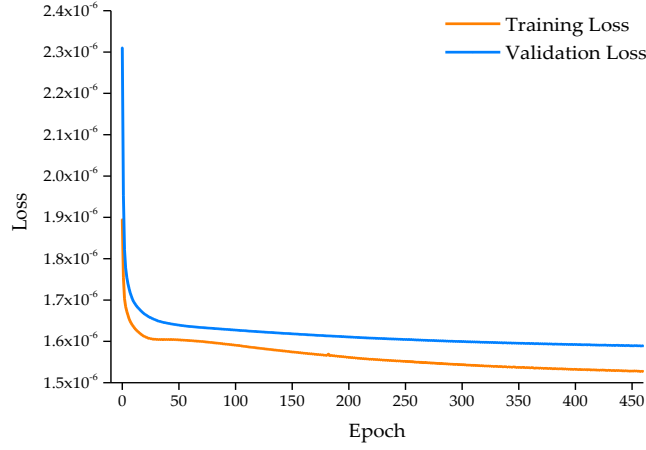
490 Two datasets from the Beijing Subway are used in the experiments, as shown in Table 4.  
491 There are 276 and 308 stations in MetroBJ2016 and MetroBJ2018, respectively. We use 25  
492 weekdays from consecutive five-week periods. The data records from MetroBJ2018 are  
493 fewer than those from MetroBJ2016 because more people entered the stations using the QR  
494 code on a mobile phone rather than swiping cards in 2018. Each record contains the card  
495 number, entry-station name, entry time, exit-station name, and the exit time. [The OD  
496 matrix and inflow/outflow series can be extracted according to Eqs. \(1\) and \(2\) every 30  
497 min.](#) All data are normalized using the min-max scaler.

498 Table 4 Data description

Description	MetroBJ2016	MetroBJ2018
Date	February 29, 2016 to April 3, 2016	October 8, 2018 to November 11, 2018
Time	05:00 to 23:00	05:00 to 23:00
Week number	5	5
Data record	130 million	110 million
Station number	276	308
Matrix dimension	276 × 276	308 × 308
Time interval	30 min	30 min
Matrix number in a day	36	36

## 499 4.2 Model configurations

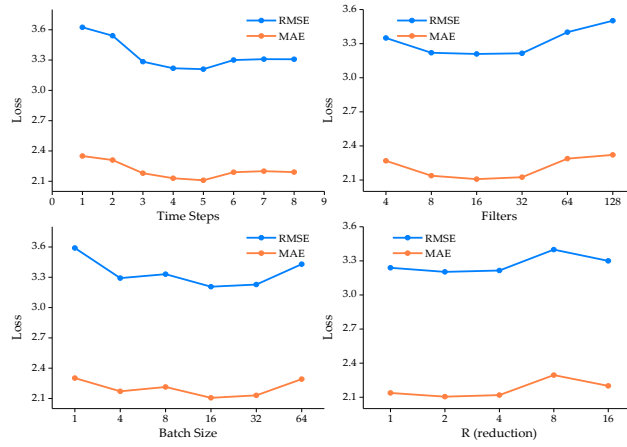
500 The data from the first four weeks are for training and validating the model, while the rest  
501 are for testing the model. The validation rate is set to 0.1. The early stopping technique is  
502 applied during model training to avoid overfitting. The training and validation losses are  
503 shown in Fig. 11. [According to the parameter tuning results, as shown in Fig. 12, we  
504 determine the hyperparameters of time steps, filters, batch size, and R \(reduction\). For the  
505 inflow/outflow-gated branch, the inflow/outflow series in the last five time steps \(2.5 h\) in  
506 the entire network are utilized. There is one layer with 16 filters for the first split CNN and  
507 one layer with one filter for the second split CNN in the trunk. The learning rate is 0.001  
508 and the batch size is 16. The tensor reduction  \$R\$  is set to two in the channel-wise attention.](#)  
509 We use the OD matrix in the same time interval in the last five days. We use the Xavier  
510 normal initializer to initialize the CNN related parameters. All models are implemented  
511 with PyTorch on a desktop computer with Intel i7-8700K processor (12M cache up to 3.20  
512 GHz), 24 GB memory, and an NVIDIA GeForce GTX 1070Ti graphics card



513

514

Fig. 11 Variation of training loss and validation loss



515

516

Fig. 12 Parameter tuning results

### 4.3 Evaluation metrics

517

518 In this study, the root-mean-squared error (RMSE), mean absolute error (MAE), and  
 519 weighted mean-absolute-percentage error (WMAPE) are chosen as evaluation metrics  
 520 according to Eqs. (13) to (15).

$$521 \quad RMSE = \sqrt{\frac{1}{(n \times n)_{no\_mask}} \sum_{i,j} (m_{ij}^{d,t} - m_{ij}^{d,t})^2} \quad (13)$$

$$522 \quad MAE = \frac{1}{(n \times n)_{no\_mask}} \sum_{i,j} \frac{|m_{ij}^{d,t} - m_{ij}^{d,t}|}{m_{ij}^{d,t}} \quad (14)$$

$$523 \quad WMAPE = \sum_{ij} \left( \frac{m_{ij}^{d,t}}{\sum_{ij} m_{ij}^{d,t}} \left| \frac{m_{ij}^{d,t} - m_{ij}^{d,t}}{m_{ij}^{d,t}} \right| \right), m_{ij}^{d,t} > 0 \quad (15)$$

524 The notations are the same as those in Eq. (9). The  $(n \times n)_{no\_mask}$  exactly indicates the OD  
 525 numbers that are not masked.

### 4.4 Benchmarks

526

527 In this section, we compare the proposed CAS-CNN model with several other models,

528 including 2D CNN, 3D CNN, ConvLSTM, ConvGRU, TrajGRU, and ST-ResNet. Moreover,  
529 we built another five models based on our model to prove the effectiveness of the proposed  
530 split CNN, the masked loss function, the channel-wise attention mechanism, and the  
531 inflow/outflow-gated mechanism. For all of them, all other parameters except the control  
532 component are the same as those in CAS-CNN. For CAS-CNN, we construct a mask file  
533 based on the low ODAD level, and apply it to the M-Loss function. The inputs and outputs  
534 are the same for all models. Note that we do not include the classical models like the  
535 historical average or autoregressive integrated moving average models in the baseline  
536 modes. Because they are unable to make predictions for a metrics (with more than 76,176  
537 OD pairs) using only one model. The detailed information for each benchmark is listed as  
538 follows.

539 **2D CNN and 3D CNN:** Both of them have three layers with 8, 16, and 1 filters, respectively.

540 The activation function for the first two layers is ReLU and the last layer is linear. The  
541 kernel size is 5×5. The learning rate is 0.001. The batch size is 8.

542 **ConvLSTM** (Xingjian *et al.*, 2015) **and ConvGRU** (Shi *et al.*, 2017): Both of them have three  
543 layers with 8, 8, and 1 filters, respectively. The kernel size is 3×3. The learning rate is  
544 0.001. The batch size is 8.

545 **TrajGRU** (Shi *et al.*, 2017): This is an encoder–forecaster architecture. There are two layers  
546 with 32 and 64 filters, respectively, in the encoder part. There are two layers with 64  
547 and 32 filters, respectively, in the forecaster part. The respective kernel sizes are 3×3  
548 and 5×5. The learning rate is 0.0001. The batch size is 16.

549 **ST-ResNet** (Zhang *et al.*, 2017): We use the residual block similar as one branch of the  
550 original ST-ResNet.

551 **CAS-CNN (No S-CNN):** We replace the split CNN with general CNN to prove the  
552 effectiveness of the split CNN. The kernel size is 3×3 in the general CNN.

553 **CAS-CNN (No Mask):** We replace the M-Loss with the general MSE loss function to prove  
554 the effectiveness of the M-Loss.

555 **CAS-CNN (No CA):** We delete the channel-wise attention mechanism to prove the  
556 effectiveness of the mechanism.

557 **CAS-CNN (No Inflow):** We delete the inflow-gated branch to prove the effectiveness of  
558 the inflow-gated mechanism.

559 **CAS-CNN (No Outflow):** We delete the outflow-gated branch to prove the effectiveness  
560 of the outflow-gated mechanism.

561 **CAS-CNN:** The whole model we propose in section 3.3.

## 562 4.5 Results and discussions

### 563 4.5.1 Network-wide prediction performance

564 The network-wide prediction performance is shown in Table 5 and Fig. 13. Several critical  
565 points can be drawn as follows:

- 566 1. It is not the more complicated the better for the deep learning models. It is the more  
567 appropriate the better. For the benchmarks, 2D CNN and 3D CNN perform similarly,  
568 and with the same regularity as those of ConvLSTM and ConvGRU. However, notably,

569 the simpler CNNs perform better than ConvLSTM and ConvGRU. Three reasons may  
570 account for this finding. First, the ConvLSTM or ConvGRU are proposed for  
571 precipitation nowcasting whose input data are denser than OD matrices in URT,  
572 especially for the matrices early in the morning or very late in the night. Second,  
573 ConvLSTM and ConvGRU are more suitable for series that have a strict chronological  
574 order. However, because the real-time OD matrices cannot be obtained in URT, the  
575 input data for this study is obtained from five former days. The chronological order is  
576 not obvious. **Third, we only have consecutive five-week AFC data. When a relatively  
577 complicated method is trained, more data is necessary. Therefore, a simpler model  
578 might perform relatively better when the data volume is limited.** Moreover, the  
579 TrajGRU, which is the most complex baseline model has the worst performance. This  
580 is because the TrajGRU is mainly designed for location-variant motion patterns that  
581 may not be suitable for OD matrices in URT. These results indicate that increased  
582 complexity might be not beneficial for the deep-learning models. Increased  
583 appropriateness is more beneficial.

584 2. **The proposed inflow/outflow-gated mechanism is conducive to improve the  
585 prediction performance. This indicates that the use of inflow/outflow series to replace  
586 the real-time OD matrices and to provide real-time information is effective. From the  
587 CAS-CNN (No Inflow/Outflow) to CAS-CNN, the RMSE is improved for  
588 MetroBJ2016 and MetroBJ2018 by 0.84% and by 1.90%, respectively. These values  
589 denote average improvements for an individual OD flow. From the network point-of-  
590 view, it is a significant improvement because there are many OD pairs in a single time  
591 interval and there are ten million passengers taking the subway in one day in Beijing,  
592 China.**

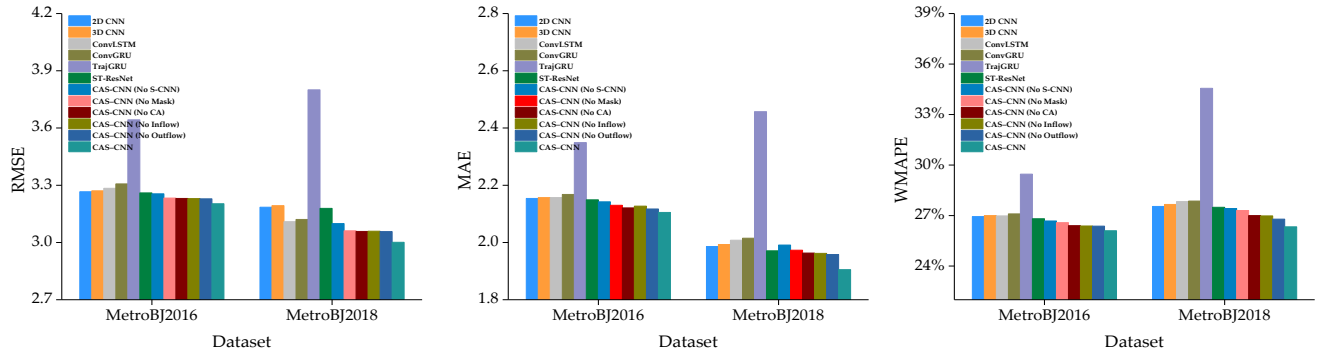
593 3. **The proposed split CNN, the masked loss function, and the channel-wise attention  
594 mechanism are also proved to be effective for model performance. This shows that  
595 deliberately dealing with small or zero flows contributes to the improvement of model  
596 performance. From the CAS-CNN (No S-CNN) to CAS-CNN, the RMSE is improved  
597 for MetroBJ2016 and MetroBJ2018 by 1.60% and by 3.16%, respectively. From the  
598 CAS-CNN (No Mask) to CAS-CNN, the RMSE is improved for MetroBJ2016 and  
599 MetroBJ2018 by 0.93% and by 1.96%, respectively. From the CAS-CNN (No CA) to  
600 CAS-CNN, the RMSE is improved for MetroBJ2016 and MetroBJ2018 by 0.87% and  
601 by 1.86%, respectively. Irrespective of the case, the CAS-CNN performs the best,  
602 which benefits from the architecture of split CNN, channel-wise attention mechanism,  
603 inflow/outflow-gated mechanism, and the masked loss function.**

604  
605  
606  
607  
608  
609  
610

Table 5 Comparison of performances of different models

Models	MetroBJ2016			MetroBJ2018		
	RMSE	MAE	WMAPE	RMSE	MAE	WMAPE
2D CNN	3.266	2.154	26.94%	3.185	1.986	27.54%
3D CNN	3.271	2.157	27.00%	3.193	1.993	27.66%
ConvLSTM	3.284	2.157	26.98%	3.109	2.008	27.83%
ConvGRU	3.307	2.168	27.10%	3.121	2.015	27.86%
TrajGRU	3.643	2.349	29.46%	3.800	2.457	34.56%
ST-ResNet	3.260	2.149	26.81%	3.179	1.971	27.49%
CAS-CNN (No S-CNN)	3.255	2.142	26.68%	3.099	1.991	27.42%
CAS-CNN (No Mask)	3.233	2.130	26.58%	3.061	1.973	27.30%
CAS-CNN (No CA)	3.231	2.121	26.40%	3.058	1.963	27.00%
CAS-CNN (No Inflow)	3.230	2.127	26.38%	3.059	1.962	26.98%
CAS-CNN (No Outflow)	3.229	2.117	26.37%	3.057	1.958	26.79%
<b>CAS-CNN</b>	<b>3.203</b>	<b>2.105</b>	<b>26.10%</b>	<b>3.001</b>	<b>1.905</b>	<b>26.33%</b>

612



613

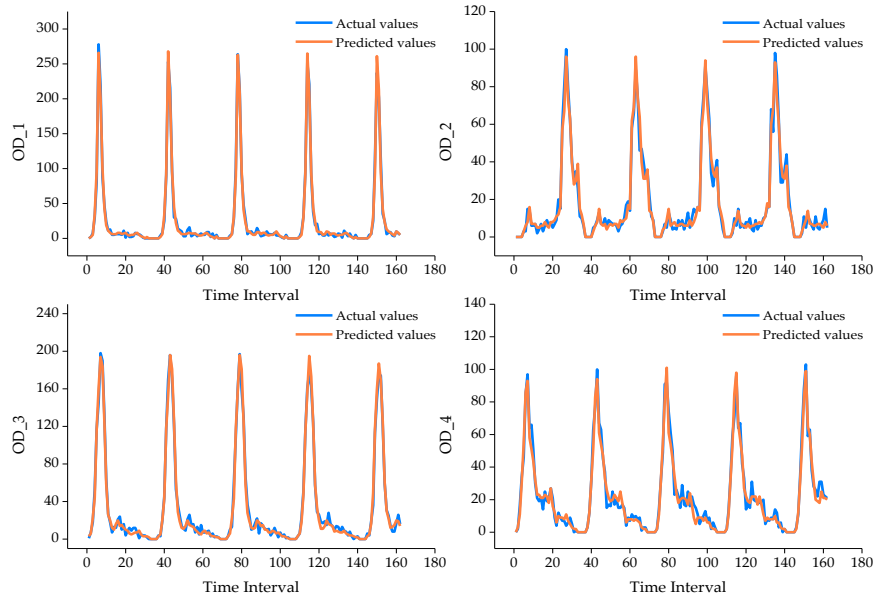
614

Fig. 13 Comparison of performances of different models

615

#### 4.5.2 Prediction performances of individual OD pairs

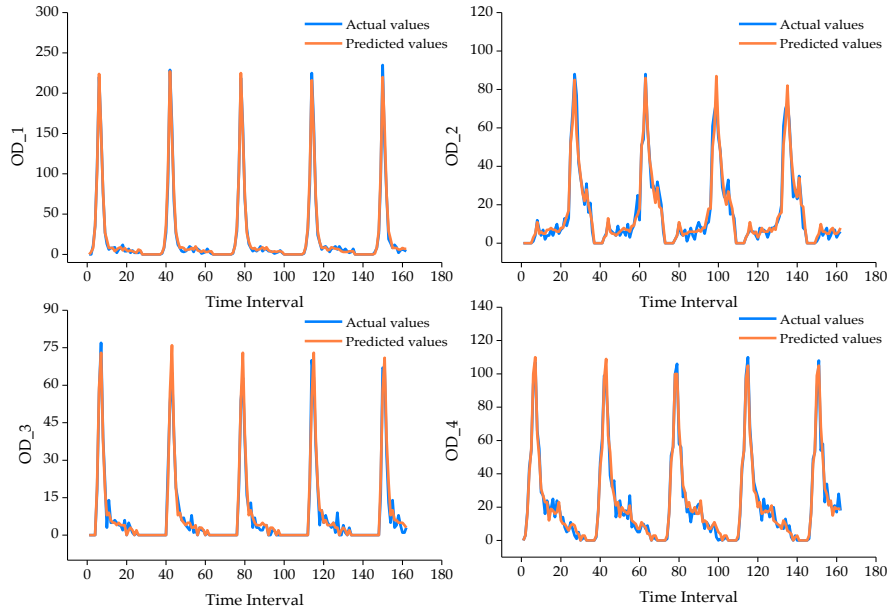
616 To evaluate models on individual OD flows, we choose several OD flows to compare the  
617 actual values and predicted values, as shown in Fig. 14 and Fig. 15. As is shown, OD\_1 is  
618 an OD flow with peak features in the morning hours. No matter for MetroBJ2016 or  
619 MetroBJ2018, the CAS-CNN can accurately capture the variation throughout a day. Even  
620 the peak flows can be predicted accurately. For OD\_2 and OD\_4, one is an OD flow with  
621 peak features in the morning hours, and the other with peak features in the evening hours.  
622 Both of them exhibit significant variations throughout the day. However, it can be  
623 observed that the trend can be captured even under the case of significant variations. For  
624 OD\_3, the flows undergone large volume reductions from 2016 to 2018, resulting in some  
625 flows in off-peak hours are masked. As is shown in Fig. 15, even when the flows in some  
626 time intervals are masked, the CAS-CNN model performs well throughout the day. In  
627 summary, the proposed CAS-CNN can perform well on an individual level in most cases  
628 in two real-world subway datasets.



629

630

Fig. 14 Comparison of actual and predicted flows of four randomly selected OD pairs in MetroBJ2016



631

632

Fig. 15 Comparison of actual and predicted flows of four randomly selected OD pairs in MetroBJ2018

633

### 4.5.3 Prediction performance in different time intervals

634

To evaluate the models in different time intervals, we calculate the average prediction accuracy at each time interval. The trend of the average evaluation metrics with time is shown in Fig. 16. In particular, there are flow vibrations at 02:00 pm, thus leading to the change of the prediction accuracies for all models. Therefore, we also compare the model performance during this period. The enlarged line graph from Fig. 16 is shown in Fig. 17. Several findings are listed as follows.

640

1. The performance for different models in different time intervals presents the same patterns as the overall performance. The CAS-CNN outperforms the rest whether in peak hours or off-peak hours. The results demonstrate the stability of the CAS-CNN

642

- 643 model.
- 644 2. Models perform stably in both morning and mid-night. When it comes to peak hours,
- 645 the performance gap becomes large, indicating that the CAS-CNN can capture the
- 646 ridership variation better.
- 647 3. There is flow variation from 01:30 pm to 03:00 pm, leading to the performance
- 648 variation for all models. However, the CAS-CNN performs the best by a large margin
- 649 during this period as shown in Fig. 17, indicating its strong adaptability.

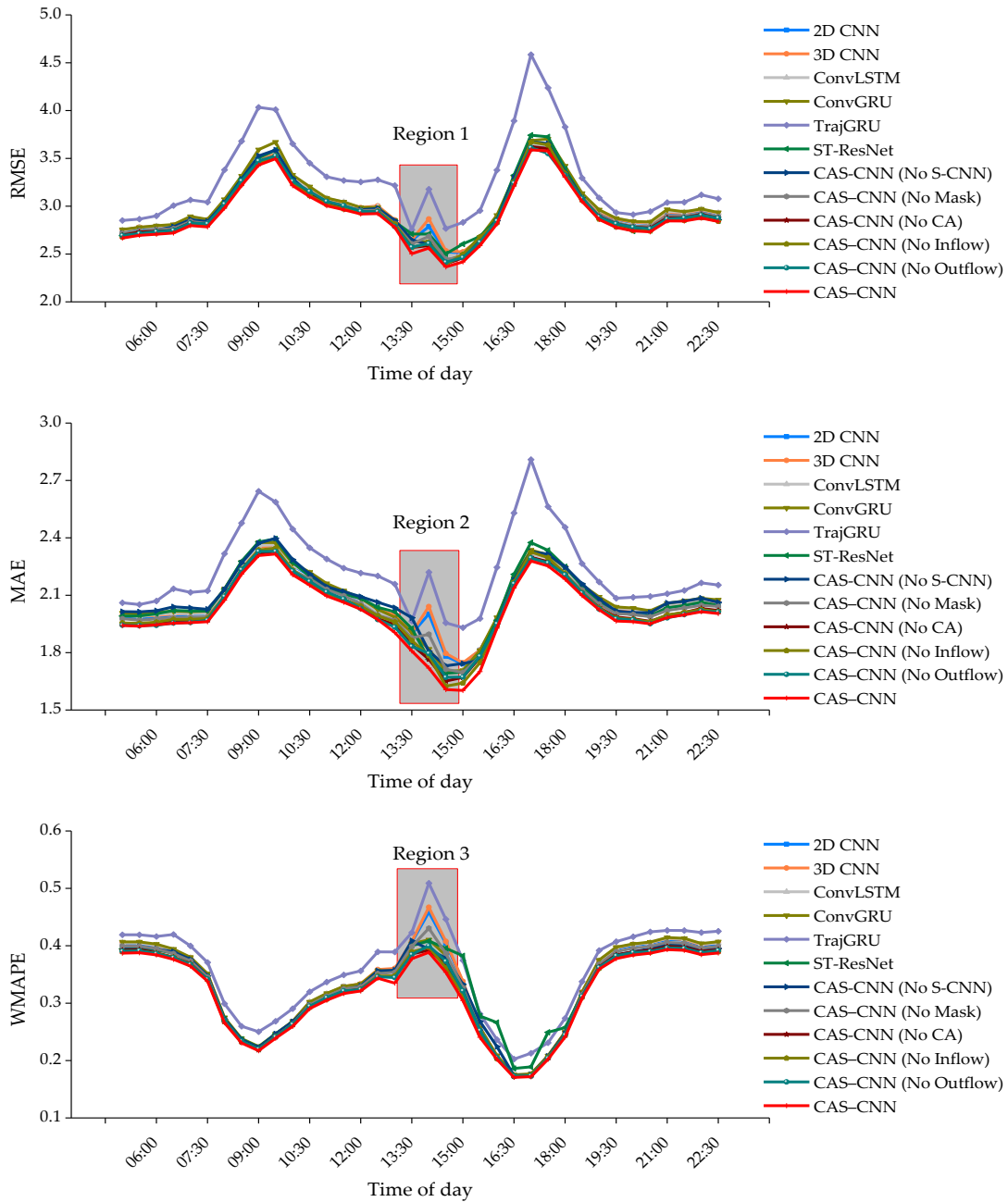


Fig. 16 Comparison of the model performance in different time intervals

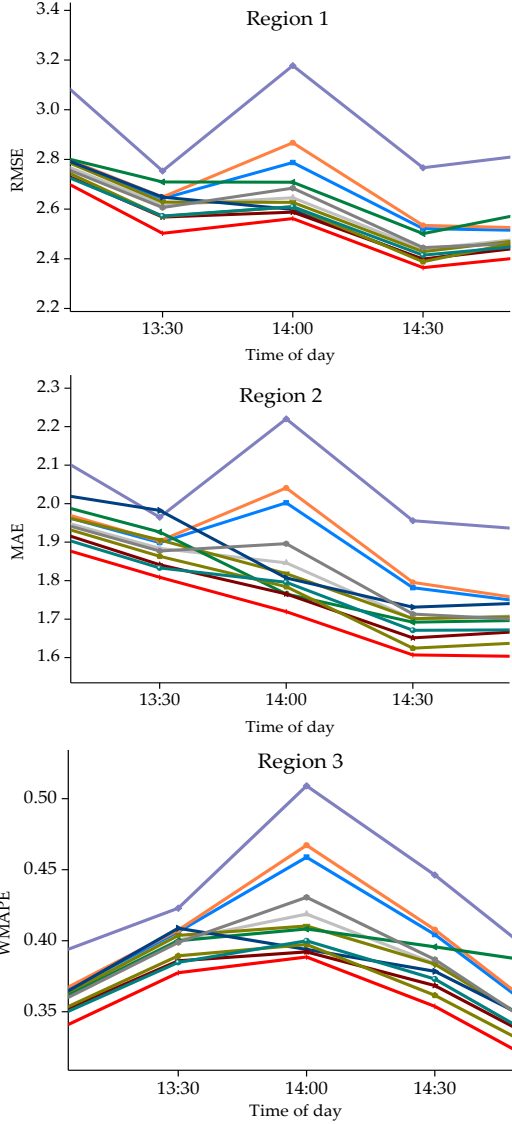


Fig. 17 Enlarged subregions from Fig. 15

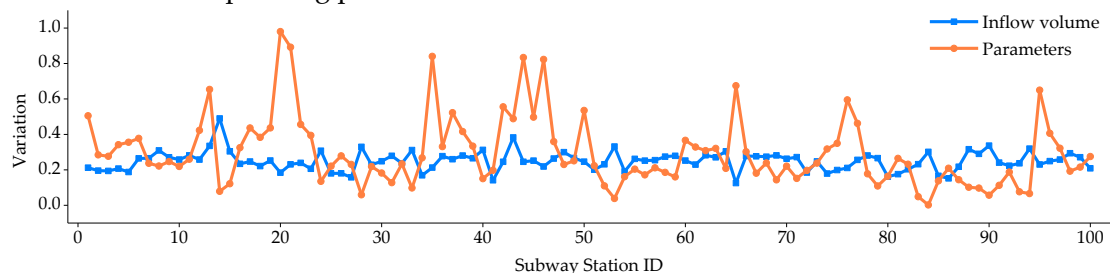
#### 4.5.4 Model interpretability

Because the real-time OD matrices are unavailable in URT, we introduce the inflow/outflow-gated mechanism to provide real-time information. To further explore the effect and the meaning of the inflow/outflow-gated mechanism, as well as the influence of small OD flows in the model, we have plotted the relationship between the inflow volume and  $w$  in Eq. (8), namely, the gated parameters, as shown in Fig. 18. For convenience, we choose 100 stations and the corresponding parameters to display. The parameters are the final trained ones. The inflow volume is the sum of inflows from the corresponding subway station. They are normalized using the min-max scaler.

As is clearly shown, there is an obvious negative correlation between the two series. This also proves the effect and the meaning of the proposed inflow-gated mechanism. Two reasons can account for this. First, the inflow-gated mechanism is mainly designed to control the output of the trunk. Therefore, the parameter size represents the strength of the control. Second, small OD flows always produce large errors. To reduce the errors, the



672 branch needs to adjust the small flows as more as possible. However, for large OD flows,  
 673 it is unnecessary to make large adjustments. Therefore, the larger the inflow volume is, the  
 674 smaller the corresponding parameter is.



675

676 Fig. 18 Relationship between the inflow volume and the gated parameters

676

## 677 5 Conclusions

678 This study proposes a channel-wise attentive split convolutional neural network (CAS-  
 679 CNN) model to conduct short-term OD prediction in URT. The proposed model consists  
 680 of various novel components, such as the split CNN, the channel-wise attention  
 681 mechanism, inflow/outflow-gated mechanism, and the masked loss function to address  
 682 the unique issues that lie in the URT OD prediction. In particular, the proposed model is  
 683 able to address the serious data sparsity issue with the use of a user-specified mask. The  
 684 split CNN is also able to obtain dense information from sparse OD matrices. To the best of  
 685 our knowledge, this is the first time that the split CNN is applied to short-term OD  
 686 prediction in URT. Given that the real-time OD matrices in URT are unavailable, we  
 687 innovatively introduce an inflow/outflow-gated mechanism to merge the historical OD  
 688 demand information with real-time inflow/outflow information. The main findings of the  
 689 study are summarized as follows:

- 690 1. Deep-learning models are becoming increasingly complex recently. Results show  
 691 that models are not the more complicated the better. It is the more appropriate the  
 692 better.
- 693 2. The data sparsity and data dimensionality issues of OD flow are critical problems  
 694 that need to be solved in URT. The proposed split CNN is able to produce dense  
 695 information from sparse OD flows. The proposed masked loss function is proved  
 696 to be effective in improving the prediction accuracy when the OD flow under low  
 697 ODAD level is masked.
- 698 3. Real-time OD flow information is unavailable because of the trip duration time.  
 699 The originally introduced inflow/outflow-gated mechanism can process the real-  
 700 time inflow/outflow information and merge them with the historical OD  
 701 information, and it improves model performance. In addition, the developed  
 702 gated mechanism demonstrates good model interpretability.
- 703 4. The CAS-CNN model demonstrates strong stability and adaptability in different  
 704 time intervals, especially under the case of flow variations.

705 Overall, these findings can provide critical insights for real-time subway operation  
 706 and management. In the future, multi-source data (weather conditions, road congestion,

707 accidents) can be used to further improve the prediction accuracy. [How to determine the](#)  
708 [threshold values of the ODAD levels is also an issue to be explored.](#) Time information such  
709 [as time of the day and day of the week can also be considered to improve the performance.](#)  
710 Besides, the OD flow prediction issue on the weekends needs to be addressed owing to the  
711 different travel patterns. More methods can be explored to address the data sparsity issue  
712 and the lack of real-time information in short-term OD prediction in the URT system.

## 713 **Conflicts of Interest**

714 The authors declare no conflict of interest.

## 715 **Acknowledgments**

716 We wish to thank the anonymous reviewers for the valuable comments, suggestions, and  
717 discussions. This work was supported by the National Natural Science Foundation of  
718 China (Project No. 71871010 and 71871027), and the grant funded by the Hong Kong  
719 Polytechnic University (Project No. P0033933) .

## 720 **References**

- 721 Chai, D., Wang, L. & Yang, Q. (2018), "Bike flow prediction with multi-graph convolutional  
722 networks", in *Proceedings of the 26th ACM SIGSPATIAL International Conference on Advances*  
723 *in Geographic Information Systems*, ACM, pp. 397-400.
- 724 Chen, L., Zhang, H., Xiao, J., Nie, L., Shao, J., Liu, W. & Chua, T. (2017), "Sca-cnn: Spatial and  
725 channel-wise attention in convolutional networks for image captioning", in *Proceedings of*  
726 *the IEEE conference on computer vision and pattern recognition*, pp. 5659-5667.
- 727 Chen, Z., Mao, B., Bai, Y., Xu, Q. & Zhang, T. (2017), "Short-term Origin-destination Estimation  
728 for Urban Rail Transit Based on Multiple Temporal Scales", *Journal of Transportation Systems*  
729 *Engineering and Information Technology*, Vol. 17 No. 5, pp. 166-172.
- 730 Cui, Z., Henrickson, K., Ke, R. & Wang, Y. (2019), "Traffic graph convolutional recurrent neural  
731 network: A deep learning framework for network-scale traffic learning and forecasting",  
732 *IEEE Transactions on Intelligent Transportation Systems*.
- 733 Cui, Z., Ke, R., Pu, Z. & Wang, Y. (2020), "Stacked bidirectional and unidirectional LSTM  
734 recurrent neural network for forecasting network-wide traffic state with missing values",  
735 *Transportation Research Part C: Emerging Technologies*, Vol. 118102674.
- 736 Geng, X., Li, Y., Wang, L., Zhang, L., Yang, Q., Ye, J. & Liu, Y. (2019), "Spatiotemporal multi-  
737 graph convolution network for ride-hailing demand forecasting", in *2019 AAAI Conference*  
738 *on Artificial Intelligence*, pp. 1-8.
- 739 Guo, G. & Yuan, W. (2020), "Short-term traffic speed forecasting based on graph attention  
740 temporal convolutional networks", *Neurocomputing*, Vol. 410, pp. 387-393.
- 741 Guo, G. & Zhang, T. (2020), "A residual spatio-temporal architecture for travel demand  
742 forecasting", *Transportation Research Part C: Emerging Technologies*, Vol. 115102639.
- 743 Guo, S., Lin, Y., Feng, N., Song, C. & Wan, H. (2019), "Attention Based Spatial-Temporal Graph  
744 Convolutional Networks for Traffic Flow Forecasting", in *2019 AAAI Conference on Artificial*

745 *Intelligence*, pp. 922-929.

746 Han, Wang, J., Ren, Gao & Chen (2019), "Predicting Station-Level Short-Term Passenger Flow  
747 in a Citywide Metro Network Using Spatiotemporal Graph Convolutional Neural  
748 Networks", *International Journal of Geo-Information*, Vol. 8, pp. 243.

749 He, K., Zhang, X., Ren, S. & Sun, J. (2015), "Deep residual learning for image recognition", in  
750 *Proceedings of the IEEE conference on computer vision and pattern recognition*, pp. 770-778.

751 Jiang, J., Lin, F., Fan, J., Lv, H. & Wu, J. (2019), "A Destination Prediction Network Based on  
752 Spatiotemporal Data for Bike-Sharing", *Complexity*, Vol. 2019.

753 Jin, G., Cui, Y., Zeng, L., Tang, H., Feng, Y. & Huang, J. (2020), "Urban ride-hailing demand  
754 prediction with multiple spatio-temporal information fusion network", *Transportation  
755 Research Part C: Emerging Technologies*, Vol. 117102665.

756 Ke, J., Qin, X., Yang, H., Zheng, Z., Zhu, Z. & Ye, J. (2019), "Predicting origin-destination ride-  
757 sourcing demand with a spatio-temporal encoder-decoder residual multi-graph  
758 convolutional network", *arXiv preprint arXiv:1910.09103*.

759 Li, L., Wang, Y., Zhong, G., Zhang, J. & Ran, B. (2018), "Short-to-medium term passenger flow  
760 forecasting for metro stations using a hybrid model", *KSCE Journal of Civil Engineering*, Vol.  
761 22 No. 5, pp. 1937-1945.

762 Lin, P. & Chang, G. (2007), "A generalized model and solution algorithm for estimation of the  
763 dynamic freeway origin-destination matrix", *Transportation Research Part B: Methodological*,  
764 Vol. 41 No. 5, pp. 554-572.

765 Liu, L., Chen, J., Wu, H., Zhen, J., Li, G. & Lin, L. (2020), "Physical-virtual collaboration graph  
766 network for station-level metro ridership prediction", *arXiv preprint arXiv:2001.04889*.

767 Liu, L., Qiu, Z., Li, G., Wang, Q., Ouyang, W. & Lin, L. (2019), "Contextualized Spatial-Temporal  
768 Network for Taxi Origin-Destination Demand Prediction", *IEEE Transactions on Intelligent  
769 Transportation Systems*.

770 Liu, Y., Liu, Z. & Jia, R. (2019), "DeepPF: A deep learning based architecture for metro passenger  
771 flow prediction", *Transportation Research Part C: Emerging Technologies*, Vol. 101, pp. 18-34.

772 Lv, Y., Duan, Y., Kang, W., Li, Z. & Wang, F. Y. (2015), "Traffic Flow Prediction With Big Data:  
773 A Deep Learning Approach", *IEEE Transactions on Intelligent Transportation Systems*, Vol.  
774 16 No. 2, pp. 865-873.

775 Ma, X., Dai, Z., He, Z., Ma, J., Wang, Y. & Wang, Y. (2017), "Learning traffic as images: a deep  
776 convolutional neural network for large-scale transportation network speed prediction",  
777 *Sensors*, Vol. 17 No. 4, pp. 818.

778 Ma, X., Tao, Z., Wang, Y., Yu, H. & Wang, Y. (2015), "Long short-term memory neural network  
779 for traffic speed prediction using remote microwave sensor data", *Transportation Research  
780 Part C: Emerging Technologies*, Vol. 54, pp. 187-197.

781 Ma, X., Zhong, H., Li, Y., Ma, J., Cui, Z. & Wang, Y. (2020), "Forecasting transportation network  
782 speed using deep capsule networks with nested lstm models", *IEEE Transactions on  
783 Intelligent Transportation Systems*.

784 Ma, Y., Kuik, R. & van Zuylen, H. J. (2013), "Day-to-Day Origin-Destination Tuple Estimation  
785 and Prediction with Hierarchical Bayesian Networks Using Multiple Data Sources",  
786 *Transportation Research Part C: Emerging Technologies*, Vol. 2343 No. 1, pp. 51-61.

787 Ou, J., Lu, J., Xia, J., An, C. & Lu, Z. (2019), "Learn, Assign, and Search: Real-Time Estimation

788 of Dynamic Origin-Destination Flows Using Machine Learning Algorithms", *IEEE Access*,  
789 Vol. 7, pp. 26967-26983.

790 Shi, X., Gao, Z., Lausen, L., Wang, H., Yeung, D., Wong, W. & Woo, W. (2017), "Deep learning  
791 for precipitation nowcasting: A benchmark and a new model", in *Advances in neural*  
792 *information processing systems*, pp. 5617-5627.

793 Sun, L. & Chen, X. (2019), "Bayesian temporal factorization for multidimensional time series  
794 prediction", *arXiv preprint arXiv:1910.06366*.

795 Szegedy, C., Liu, W., Jia, Y., Sermanet, P., Reed, S., Anguelov, D., Erhan, D., Vanhoucke, V. &  
796 Rabinovich, A. (2015), "Going deeper with convolutions", in *Proceedings of the IEEE*  
797 *conference on computer vision and pattern recognition*, pp. 1-9.

798 Szegedy, C., Vanhoucke, V., Ioffe, S., Shlens, J. & Wojna, Z. (2016), "Rethinking the inception  
799 architecture for computer vision", in *Proceedings of the IEEE conference on computer vision and*  
800 *pattern recognition*, pp. 2818-2826.

801 Vaswani, A., Shazeer, N., Parmar, N., Uszkoreit, J., Jones, L., Gomez, A. N., Kaiser, A. &  
802 Polosukhin, I. (2017), "Attention is all you need", in *Advances in neural information processing*  
803 *systems*, pp. 5998-6008.

804 Vlahogianni, E. I., Karlaftis, M. G. & Golias, J. C. (2014), "Short-term traffic forecasting: Where  
805 we are and where we're going", *Transportation Research Part C: Emerging Technologies*, Vol.  
806 4, pp. 33-19.

807 Wang, F., Jiang, M., Qian, C., Yang, S., Li, C., Zhang, H., Wang, X. & Tang, X. (2017), "Residual  
808 attention network for image classification", in *Proceedings of the IEEE conference on computer*  
809 *vision and pattern recognition*, pp. 3156-3164.

810 Wang, S., Ou, D., Dong, D. & Xie, H. (2011), "Research on the model and algorithm of origin-  
811 destination matrix estimation for urban rail transit", in *Proceedings 2011 International*  
812 *Conference on Transportation, Mechanical, and Electrical Engineering (TMEE)*, IEEE, pp. 1403-  
813 1406.

814 Wang, Y., Yin, H., Chen, H., Wo, T., Xu, J. & Zheng, K. (2019), "Origin-Destination Matrix  
815 Prediction via Graph Convolution: a New Perspective of Passenger Demand Modeling",  
816 in *Proceedings of the 25th ACM SIGKDD International Conference on Knowledge Discovery &*  
817 *Data Mining*, ACM, pp. 1227-1235.

818 Wei, Y. & Chen, M. C. (2012), "Forecasting the short-term metro passenger flow with empirical  
819 mode decomposition and neural networks", *Transportation Research Part C Emerging*  
820 *Technologies*, Vol. 21 No. 1, pp. 148-162.

821 Xi, J., Fei-Fan, J. & Jia-Ping, F. (2018), "An Online Estimation Method for Passenger Flow OD of  
822 Urban Rail Transit Network by Using AFC Data", *Journal of Transportation Systems*  
823 *Engineering and Information Technology*, Vol. 18 No. 5, pp. 129-135.

824 Xingjian, S., Chen, Z., Wang, H., Yeung, D., Wong, W. & Woo, W. (2015), "Convolutional LSTM  
825 network: A machine learning approach for precipitation nowcasting", in *Advances in neural*  
826 *information processing systems*, pp. 802-810.

827 Xiong, X., Ozbay, K., Jin, L. & Feng, C. (2019), "Dynamic Prediction of Origin-Destination Flows  
828 Using Fusion Line Graph Convolutional Networks", *arXiv preprint arXiv:1905.00406*.

829 Xu, M., Dai, W., Liu, C., Gao, X., Lin, W., Qi, G. & Xiong, H. (2020), "Spatial-Temporal  
830 Transformer Networks for Traffic Flow Forecasting", *arXiv preprint arXiv:2001.02908*.

- 831 Yang, C., Yan, F. & Xu, X. (2017), "Daily metro origin-destination pattern recognition using  
832 dimensionality reduction and clustering methods", in *2017 IEEE 20th International  
833 Conference on Intelligent Transportation Systems (ITSC)*, IEEE, pp. 548-553.
- 834 Yang, H., Iida, Y. & Sasaki, T. (1991), "An analysis of the reliability of an origin-destination trip  
835 matrix estimated from traffic counts", *Transportation Research Part B: Methodological*, Vol. 25  
836 No. 5, pp. 351-363.
- 837 Yang, Z., Yang, D., Dyer, C., He, X., Smola, A. & Hovy, E. (2016), "Hierarchical attention  
838 networks for document classification", in *Proceedings of the 2016 conference of the North  
839 American chapter of the association for computational linguistics: human language technologies*,  
840 pp. 1480-1489.
- 841 Yao, H., Tang, X., Wei, H., Zheng, G. & Li, Z. (2019), "Revisiting Spatial-Temporal Similarity: A  
842 Deep Learning Framework for Traffic Prediction", in *2019 AAAI Conference on Artificial  
843 Intelligence*, pp. 1-8.
- 844 Yao, X. M., ZHAO, P. & Yu, D. D. (2015), "Real-time origin-destination matrices estimation for  
845 urban rail transit network based on structural state-space model", *Journal of Central South  
846 University*, Vol. 22 No. 11, pp. 4498-4506.
- 847 Yao, X. M., ZHAO, P. & Yu, D. D. (2016), "Dynamic origin-destination matrix estimation for  
848 urban rail transit based on averaging strategy", *Journal of Jilin University (Engineering and  
849 Technology Edition)*, Vol. 46 No. 1, pp. 92-99.
- 850 Yu, B., Yin, H. & Zhu, Z. (2017), "Spatio-temporal graph convolutional networks: A deep  
851 learning framework for traffic forecasting", *arXiv preprint arXiv:1709.04875*.
- 852 Yu, R., Wang, Y., Zou, Z. & Wang, L. (2020), "Convolutional neural networks with refined loss  
853 functions for the real-time crash risk analysis", *Transportation Research Part C: Emerging  
854 Technologies*, Vol. 119102740.
- 855 Zhang, J., Chen, F. & Shen, Q. (2019), "Cluster-Based LSTM Network for Short-Term Passenger  
856 Flow Forecasting in Urban Rail Transit", *IEEE Access*, Vol. 7, pp. 147653-147671.
- 857 Zhang, J., Chen, F., Cui, Z., Guo, Y. & Zhu, Y. (2020), "Deep Learning Architecture for Short-  
858 Term Passenger Flow Forecasting in Urban Rail Transit", *IEEE Transactions on Intelligent  
859 Transportation Systems*.
- 860 Zhang, J., Chen, F., Guo, Y. & Li, X. (2020a), "Multi-Graph Convolutional Network for Short-  
861 Term Passenger Flow Forecasting in Urban Rail Transit", *IET Intelligent Transport Systems*,  
862 Vol. 14 No. 10, pp. 1210-1217..
- 863 Zhang, J., Chen, F., Wang, Z. & Liu, H. (2019), "Short-Term Origin-Destination Forecasting in  
864 Urban Rail Transit Based on Attraction Degree", *IEEE Access*, Vol. 7, pp. 133452-133462.
- 865 Zhang, J., Shen, D., Tu, L., Zhang, F., Xu, C., Wang, Y., Tian, C., Li, X., Huang, B. & Li, Z. (2017),  
866 "A real-time passenger flow estimation and prediction method for urban bus transit  
867 systems", *IEEE Transactions on Intelligent Transportation Systems*, Vol. 18 No. 11, pp. 3168-  
868 3178.
- 869 Zhang, J., Zheng, Y. & Qi, D. (2017), "Deep spatio-temporal residual networks for citywide  
870 crowd flows prediction", in *2017 AAAI Conference on Artificial Intelligence*, pp. 1-7.
- 871 Zhang, K., Jia, N., Zheng, L. & Liu, Z. (2019), "A novel generative adversarial network for  
872 estimation of trip travel time distribution with trajectory data", *Transportation Research Part  
873 C: Emerging Technologies*, Vol. 108, pp. 223-244.

- 874 Zhang, T. & Guo, G. (2020), "Graph Attention LSTM: A Spatio-Temporal Approach for Traffic  
875 Flow Forecasting", *IEEE Intelligent Transportation Systems Magazine*.
- 876 Zhao, J., Rahbee, A. & Wilson, N. H. (2007), "Estimating a Rail Passenger Trip Origin-  
877 Destination Matrix Using Automatic Data Collection Systems", *Computer-Aided Civil and*  
878 *Infrastructure Engineering*, Vol. 22 No. 5, pp. 376-387.
- 879 Zhou, H., Tan, L., Zeng, Q. & Wu, C. (2016), "Traffic matrix estimation: A neural network  
880 approach with extended input and expectation maximization iteration", *Journal of Network*  
881 *and Computer Applications*, Vol. 60, pp. 220-232.